

# Temperature Dependence of Dielectric Properties in Doped Perovskites

Vijendra Lingwal<sup>1</sup>, A S Kandari<sup>2</sup> & N S Panwar<sup>3</sup>

<sup>1</sup>Department of Physics, Pt. L.M.S. Govt. PG College Rishikesh, Dehradun, Uttarakhand, India

<sup>2</sup>Department of Physics, Govt. PG College New Tehri, Uttarakhand, India

<sup>3</sup>University Science Instrumentation Centre, HNB Garhwal University, Srinagar (Garhwal), India

## ABSTRACT

Pellet samples of mixed sodium-potassium tantalate ( $\text{Na}_{1-x}\text{K}_x\text{TaO}_3$ ), for compositions  $x = 0, 0.2$  and  $0.5$  were prepared by solid-state reaction method. The calcined mixture was pressed at  $0.02$  MPa and sintered in a closed furnace to form  $6$  mm diameter pellets. Temperature variation of dielectric constant and loss tangent of the prepared samples has been studied in the frequency range from  $10$  KHz to  $1$  MHz. Dielectric anomalies have been observed near the transition temperatures of the samples. Dielectric constant and loss tangent peak heights were observed decreasing with increasing frequency, for all the compositions, which show relaxational behavior of the material.

**Keywords** – Dielectric constant, loss tangent, perovskites, relaxational behavior, transition temperature.

## 1. INTRODUCTION

Study of dielectric constant and loss tangent provides insight to the understanding of intra- and inter-molecular interactions, modes of motion and configurational changes in a solid. The perovskite ( $\text{ABO}_3$ ) type alkali metal niobates and tantalates constitute an important group of oxide compounds with broad ranges of technologically important dielectric, piezoelectric, ferroelectric and optoelectronic properties<sup>1</sup>. Solid solutions of sodium potassium niobate ( $\text{Na}_{1-x}\text{K}_x\text{NbO}_3$ ) and sodium potassium tantalate ( $\text{Na}_{1-x}\text{K}_x\text{TaO}_3$ ) can be formed over the whole composition range ( $x = 0$  to  $1$ ), which allow a high degree of tailorability of physical properties. For low  $x$  values, these systems appear to exhibit true phase transitions and their dielectric properties can be understood in terms of soft optic phonons<sup>2-3</sup>.

Interest has centered on  $\text{Na}_{1-x}\text{K}_x\text{TaO}_3$  system, especially in relation to quantum effects, suppression of the phase transition and the question of long-range order vs glasslike behavior<sup>4</sup>.  $\text{Na}_{1-x}\text{K}_x\text{TaO}_3$  system has interesting end members, i.e.,  $\text{NaTaO}_3$  is ferroelectric with ilmenite structure at room temperature and a transition temperature ( $T_c$ )  $\sim 475^\circ\text{C}$ , and  $\text{KTaO}_3$  is paraelectric, at room temperature<sup>5</sup>. Na in  $\text{KTaO}_3$  occurs as an off-centre impurity and makes  $\text{KTaO}_3$  a wide gap incipient ferroelectric. Davis<sup>3</sup> has observed that, for  $x \geq 0.70$ , this system shows a single-phase transition from the high temperature cubic paraelectric phase to a tetragonal ferroelectric phase (CT). For  $0.70 \geq x \geq 0.45$ , it shows two ferroelectric transitions, a cubic to tetragonal transition followed by a lower temperature transition to a phase believed to have an orthorhombic symmetry<sup>3</sup>. Samara has found the pressure dependence of CT transition, in  $\text{Na}_{0.28}\text{K}_{0.72}\text{TaO}_3$  single crystal, consistent with the soft mode theory<sup>1</sup>.

$\text{Na}_{1-x}\text{K}_x\text{TaO}_3$  is a relatively less studied system. Investigators have studied the low temperature dielectric behavior of  $\text{Na}_{1-x}\text{K}_x\text{TaO}_3$  single crystals<sup>1,3</sup> and high temperature phases, conductivity and structure of  $\text{NaTaO}_3$  and  $\text{KTaO}_3$ <sup>6,7</sup>. In the present study dielectric measurements on  $\text{Na}_{1-x}\text{K}_x\text{TaO}_3$  pellet samples, for different  $x$  values, in the temperature range from  $50$  to  $680^\circ\text{C}$ , have been carried out.

## 2. PREPARATION

Materials were prepared with conventional solid-state reaction method. The starting materials were sodium carbonate ( $\text{Na}_2\text{CO}_3$ ) (99.95 % pure), potassium carbonate ( $\text{K}_2\text{CO}_3$ ) (99.95 % pure) and tantalum pentoxide ( $\text{Ta}_2\text{O}_5$ ) (99.95 % pure), for preparing  $\text{Na}_{1-x}\text{K}_x\text{TaO}_3$  system. The starting materials were initially dried at  $150^\circ\text{C}$  to remove the absorbed moisture.  $\text{K}_2\text{CO}_3$  is a hygroscopic material and hence due care was taken in its handling. Different compositions of  $\text{Na}_{1-x}\text{K}_x\text{TaO}_3$  ( $x = 0, 0.2$  and  $0.5$ ) were prepared by weighing the starting materials in stoichiometric ratio. Each composition was manually dry mixed for 1 hour and with methyl alcohol for another 1 hour using agate mortar and pestle. The mixture was calcined in an alumina crucible in ambient atmosphere at  $950^\circ\text{C}$  for 2 hours, to remove carbonates present in the mixture. After cooling, in dry air, the calcined mixture was weighed to ensure complete carbonate removal from the mixture. Calcined mixture was pressed at 0.02 MPa to form the pellets of 6 mm diameter. These raw pellets were sintered in a closed furnace. All the pellet samples, except  $\text{NaTaO}_3$ , were placed in an alumina crucible and sintered at  $1050^\circ\text{C}$ , for 15 hours. Due to their high melting point  $\text{NaTaO}_3$  pellets were sintered at  $1100^\circ\text{C}$ , for 15 hours. All the samples were taken out from the furnace when it cooled to room temperature.

## 3. MEASUREMENTS

Room temperature x-ray diffraction patterns of all the prepared samples were taken by Philips analytical x-ray diffractometer (PW3710), using  $\text{CuK}\alpha_1$  radiation of wavelength  $1.54056\text{\AA}$ . Peak indexing was done by using Joint Committee on Powder Diffraction Standards (JCPDS) data cards. Crystallite size of the samples was calculated from the full width at half maximum (FWHM) of the highest intensity peak in the XRD pattern<sup>8</sup> and the perovskite subcell parameters were obtained using the relation provided by Azaroff<sup>9</sup>. Sintered pellets were electroded, with air-drying silver paste, in metal-insulator-metal (MIM) configuration for dielectric measurements.

Dielectric properties of  $\text{Na}_{1-x}\text{K}_x\text{TaO}_3$  ceramics vary with  $x$  and preparation conditions. Temperature and frequency dependence of dielectric properties of  $\text{Na}_{1-x}\text{K}_x\text{TaO}_3$  system, for  $x = 0, 0.2$  and  $0.5$ , were investigated in the present study. For studying the temperature and frequency dependence of dielectric properties, measurement were made run to run on the same sample and sample to sample for all samples prepared with the similar method, in the frequency range from 10 KHz to 1 MHz, and in temperature range from 50 to  $680^\circ\text{C}$ . The observations were close to each other and the values were averaged. Capacitance and dissipation factor measurements were carried out in MIM configuration, using Fluke- PM6306 RCL meter and HP-4275 Multifrequency LCR meter. Dielectric constant ( $K$ ) was calculated by the relation,

$K = C/C_0$ ; where  $C$  and  $C_0$  are the capacitances of the electrodes with and without dielectric, respectively;  $C_0$  is given by,

$$C_0 = (0.0885 \pi r^2/d) \text{ pF}; \text{ where } r \text{ (cm) is the radius of the electrodes and } d \text{ (cm) distance between them.}$$

## 4. RESULTS AND DISCUSSION

Fig. 1 shows room temperature x-ray diffraction patterns of  $\text{Na}_{1-x}\text{K}_x\text{TaO}_3$  samples for  $x = 0, 0.2$  and  $0.5$ . The patterns show an orthorhombic polycrystalline structure with peaks corresponding to (101), (200), (220), etc. planes. The

diffraction peaks were observed shifting towards lower angle with increasing  $x$  value. Lattice parameters for  $\text{NaTaO}_3$  were obtained as  $a = 5.5228$ ,  $b = 7.7847$  and  $c = 5.5451$  Å; which were found comparable to the reported values<sup>10</sup>. Addition of potassium shows decreasing crystallite size, 0.0338, 0.0219 and 0.0108  $\mu\text{m}$  for  $x = 0, 0.2$  and 0.5, respectively, in  $\text{Na}_{1-x}\text{K}_x\text{TaO}_3$  composition. The observed decrease in the crystallite size with increasing  $x$  values, in these samples, may be due to their sintering at the same temperature. All potassium incorporated samples, in the present study, were sintered at the same temperature (at 1050 °C). However, it is worth noting that the melting point of these materials decreases with increasing potassium content<sup>11</sup> and hence ideally the sintering temperature of these compositions should be varied accordingly.

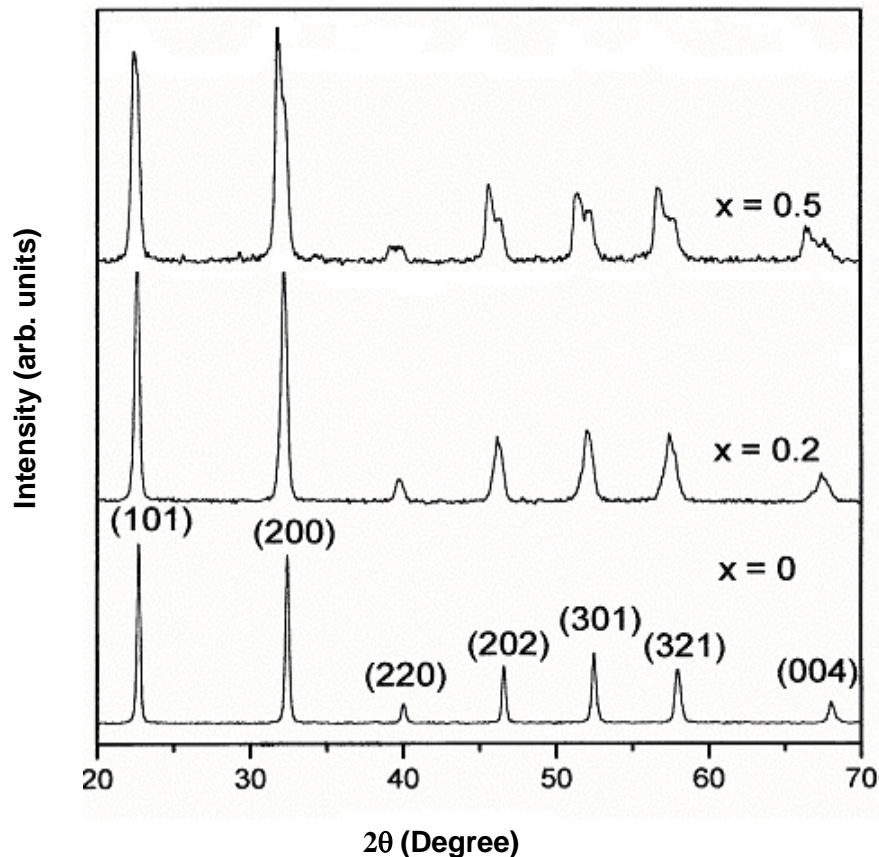


Fig. 1 - X-ray diffraction patterns of  $\text{Na}_{1-x}\text{K}_x\text{TaO}_3$  samples for different  $x$  values, at room temperature

The observed temperature variation of dielectric constant and loss tangent of  $\text{Na}_{1-x}\text{K}_x\text{TaO}_3$  system (for  $x = 0$ ) has been shown in Figs. 2 and 3. Dielectric constant remains almost constant and shows anomaly at 480 °C for all the measured frequencies. The peak value of dielectric constant was observed decreasing with increasing frequency, i.e., 277, 120 and 59; at 10, 100 and 1000 KHz, respectively. Loss tangent initially decreases up to 100 °C, remains constant between 100 and 325 °C, and thereafter increases sharply near the transition temperature. Loss tangent decreases with increasing frequency. For  $x = 0.2$ , an anomaly at 150 °C was observed in dielectric constant and loss tangent measurements, Figs. 4 and 5.

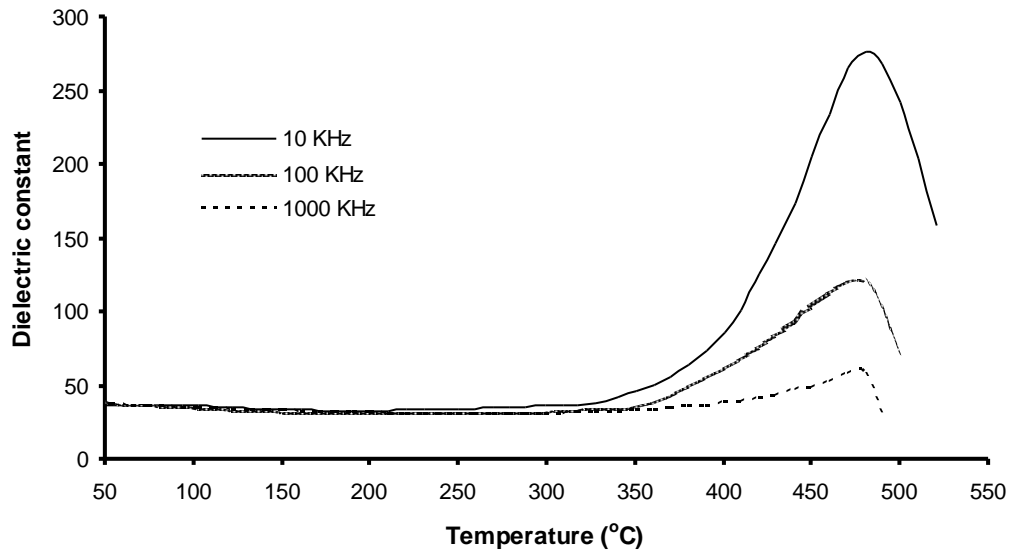


Fig. 2 Temperature dependence of dielectric constant, in  $\text{NaTaO}_3$ , at different frequencies.

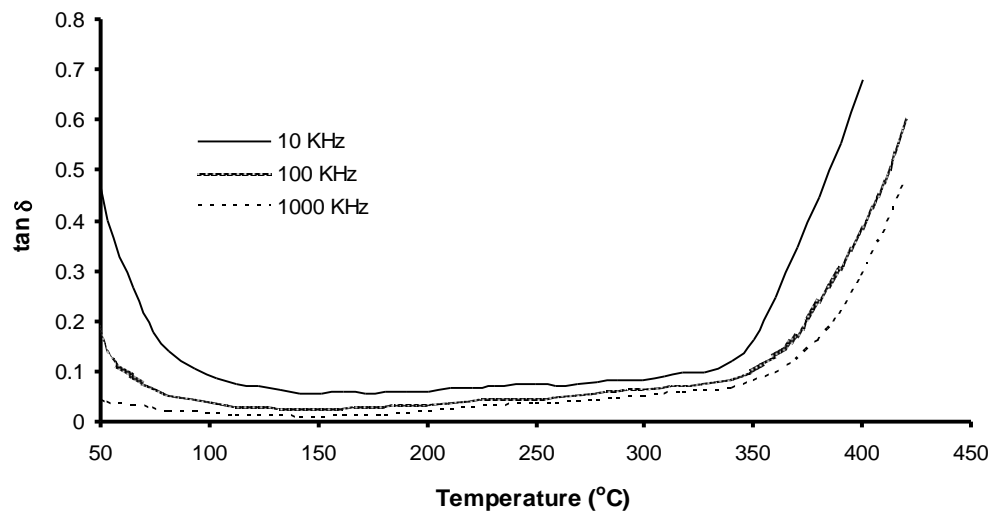


Fig. 3 Temperature dependence of loss tangent ( $\tan \delta$ ), in  $\text{NaTaO}_3$ , at different frequencies.

Temperature variation of dielectric constant and loss tangent at different frequencies for  $x = 0.5$ , in  $\text{Na}_{1-x}\text{K}_x\text{TaO}_3$  system, has been given in Figs. 6 and 7, respectively. An anomaly at  $420^\circ\text{C}$ , followed by two small peaks at  $490$  and  $631^\circ\text{C}$ , was observed in the dielectric constant measurements. These peaks may be associated with certain structural transitions at these temperatures.

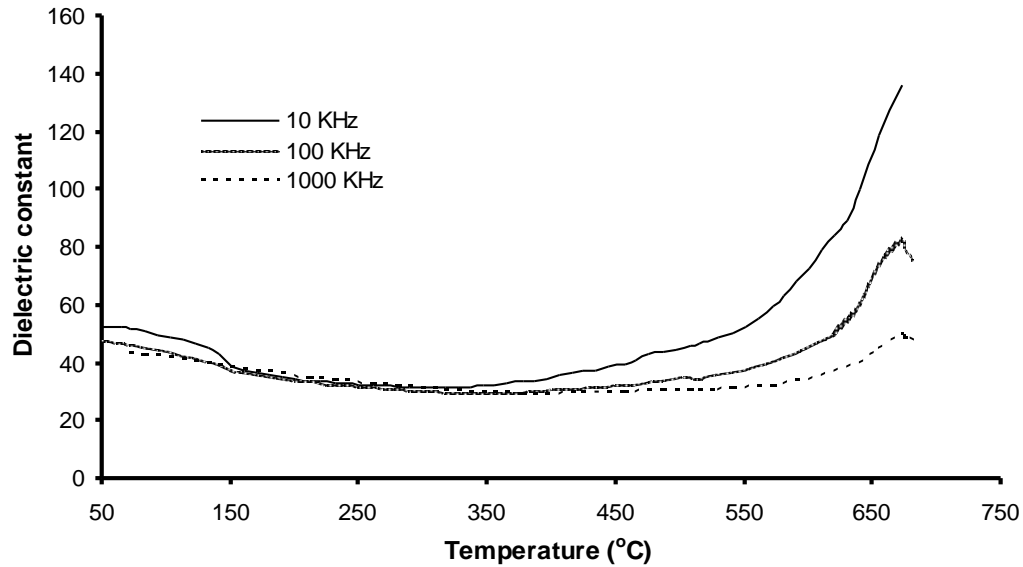


Fig. 4 Temperature dependence of dielectric constant, in  $\text{Na}_{0.8}\text{K}_{0.2}\text{TaO}_3$ , at different frequencies.

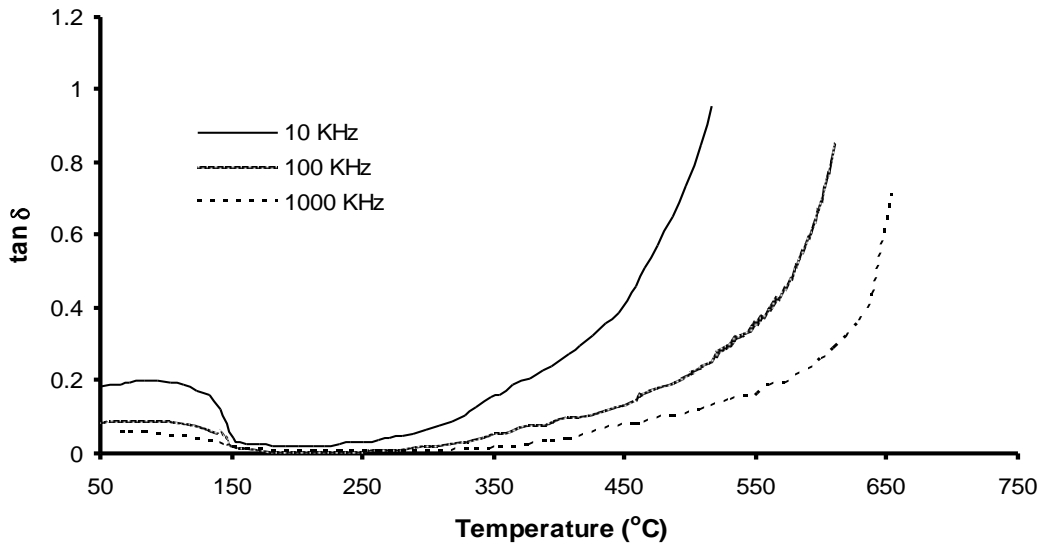


Fig. 5 Temperature dependence of loss tangent ( $\tan \delta$ ), in  $\text{Na}_{0.8}\text{K}_{0.2}\text{TaO}_3$ , at different frequencies.

Dielectric constant and loss tangent peak heights decrease with increasing frequency, in the prepared samples. Decreasing nature of dielectric constant with increasing frequency may be due to the relaxational behavior of a material<sup>12</sup>. Lossy dielectrics can be represented by the circuit analog of a resistance in parallel with a capacitor<sup>12</sup>. At higher frequency the capacitor offers low reactance to the sinusoidal signal, which minimizes the conduction losses in the resistor. Hence, the value of dielectric loss decreases at higher frequencies.

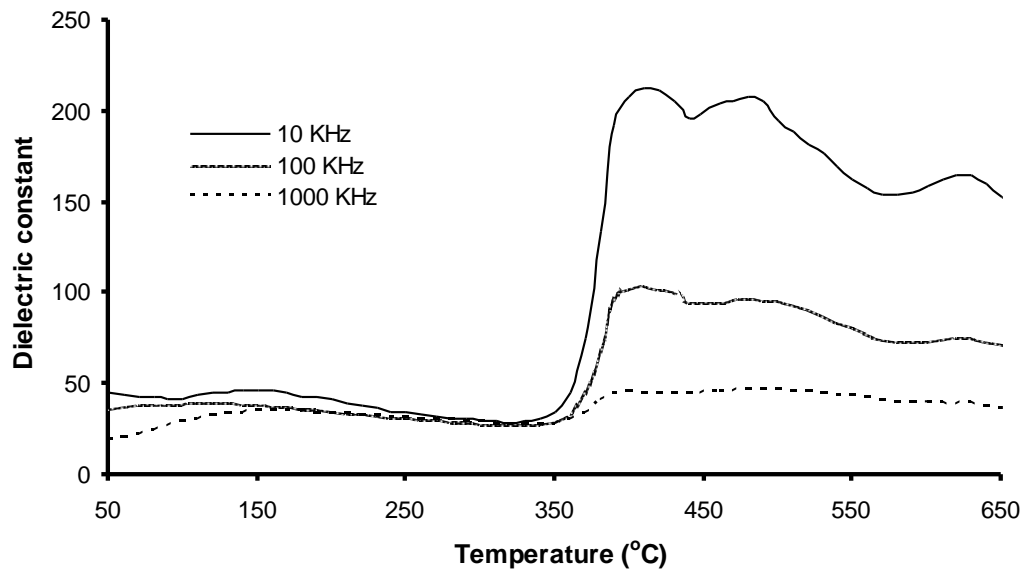


Fig. 6 Temperature dependence of dielectric constant, in  $\text{Na}_{0.5}\text{K}_{0.5}\text{TaO}_3$ , at different frequencies.

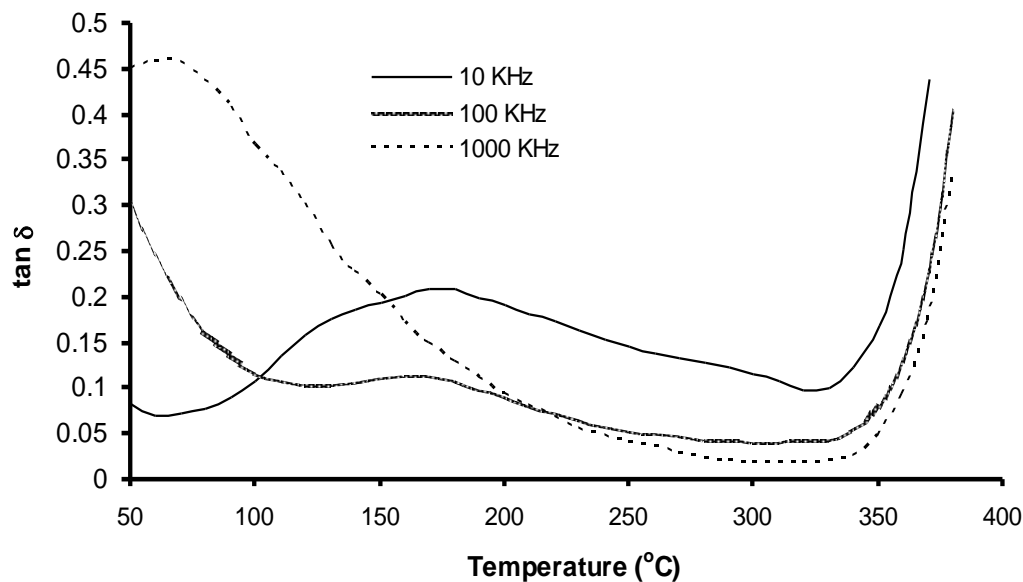


Fig. 7- Temperature dependence of loss tangent ( $\tan \delta$ ), in  $\text{Na}_{0.5}\text{K}_{0.5}\text{TaO}_3$ , at different frequencies.

The damping out of successive relaxation modes is attributed to the decrease of peak height with frequency<sup>12</sup>. The anomalous behavior at certain temperature is due to structural change or phase transition of the material at that temperature<sup>13, 14</sup>. This phase transition in the perovskite type materials is, generally, assumed to be due to the instability of temperature dependent low frequency optical phonon- the soft phonon mode, at transition temperature<sup>15</sup>. Anharmonic interactions among different modes are held responsible for the observed temperature dependence of dielectric properties<sup>14, 16</sup>. At the transition temperature, frequency of the soft mode tends to zero and

the lattice displacement associated with it becomes unstable, leading to the structural change in the lattice. The observed anomalous behavior of dielectric properties of these materials can be associated with the structural change of the lattice near the transition temperature.

The frequency dispersion or change in dielectric properties with frequency and the corresponding circuit analogs for a general solid show several relaxation modes. The dielectric constant shows an expected decrease with frequency as successive polarization modes become damped out, and corresponding peaks occur in the loss spectra at the different relaxation and resonance frequencies. The resonance losses occurring for ionic and electronic oscillations at infrared and ultraviolet frequencies are associated with absorption interactions with the incident radiation at or near the natural vibration frequencies for the ions or electrons. Relaxation losses, conversely, are associated with dipolar orientation, ion jump, or electron hopping, and can occur over a wide frequency range. Contributions to the overall dielectric constant from different polarization mechanisms are related to the composition, frequency, and temperature of the dielectric.

## 5. CONCLUSIONS

The x-ray diffraction patterns of the prepared samples show orthorhombic polycrystalline behavior. With increasing x value in  $\text{Na}_{1-x}\text{K}_x\text{TaO}_3$ , the diffraction peaks were observed shifting towards lower angle. The lattice parameters calculated from the XRD pattern, for  $\text{NaTaO}_3$ , were found comparable to the reported values<sup>10</sup>. The crystallite size was found decreasing with increasing x value, which may be due to same sintering condition for all the compositions, whereas the melting point varies with varying x value. The dielectric constant and loss tangent of the prepared samples have been found decreasing with increasing frequency, which show relaxational behavior of the material. The observed dielectric anomalies in  $\text{Na}_{1-x}\text{K}_x\text{TaO}_3$  system can be associated with the softening of the relaxational modes near transition temperatures<sup>17</sup>. Damping out of successive relaxational modes may be attributed to the decrease in dielectric peak height with increasing frequency. Dielectric constant and dielectric loss have been found lower for the present system than those for its niobate counter part<sup>1, 18-19</sup> and hence the former can be used in ultrasonic delay lines in place of the latter.

## REFERENCES

1. G.A. Samara, *Ferroelectrics*, 73 (1987), 145.
2. G.A. Samara and P. S. Peercy, *Solid State Physics* (Academic Press, New York, 1981).
3. T.G. Davis, *Phys Rev*, 5 (1972), 2530.
4. G.A. Samara, Proceedings of the 6<sup>th</sup> International Meeting on Ferroelectricity, Kobe, Japan 1985.
5. P. Vousden, *Acta Cryst*, 4 (1951), 373.
6. C.N.W. Darlington and K. S. Knight, *Acta Cryst*, 55 (1999), 24.
7. A. Arakcheeva, G. Chapuis, V. Grinevitch and V. Shamray, *Acta Cryst*, 57 (2001), 157.
8. B.D. Cullity, *Elements of X-ray Diffraction* (Addison-Wesley Publishing Company Inc., 1977).
9. L.V. Azaroff, *Elements of X-ray Crystallography* (McGraw Hill Book Company, New York, 1968).
10. H.F. Kay and J.L. Miles, *Acta Cryst*, 10 (1957), 213.

11. A. Reisman and E. Banks, *J Amer Ceram Soc*, 80 (1958), 1877.
12. G. Goodman, R.C. Buchanan and T.G. Reynolds III, *Ceramic Materials for Electronics; Processing, Properties, and Application*, Ed. Relva C Buchanan, (Marcel Dekker Inc., New York, 1991).
13. E. Pytte, *Phys Rev*, 5 (1972), 3758.
14. B.S. Semwal and N.S.Panwar, *Bull Mater Sci*, 15 (1992), 237.
15. W. Cochran, *Adv Phys*, 9 (1960), 387.
16. N.S. Panwar, T.C. Upadhyay and B.S. Semwal, *Pramana J Phys*, 33 (1989), 603.
17. Vijendra Lingwal, B.S. Semwal and N.S. Panwar, *Bull Mat Sci*, 26 (2003), 619.
18. L. Egerton and D.M. Dillon, *J Amer Ceram Soc*, 42 (1959), 438.
19. S. Narayana Murty, K.V. Rama Murty, K. Umakantham and A. Bhanumathi, *Ferroelectrics*, 102 (1990), 243.